$(LaSe)_{1.14}(NbSe_2)_2$ - a metal - insulator quantum well crystal?

1997 J. Phys.: Condens. Matter 9 10545

(http://iopscience.iop.org/0953-8984/9/47/021)

J. Phys.: Condens. Matter **9** (1997) 10545–10553. Printed in the UK PII: S0953-8984(97)84073-8

$(LaSe)_{1.14}(NbSe_2)_2$—a metal–insulator quantum well crystal?

D Berner†, H Leihenseder†, K Widder†, H P Geserich†, V M Burlakov‡, B N Mavrin‡, V N Denisov‡, R Roesky§, P Gressier§ and A Meerschaut§

† Institut für Angewandte Physik, Universität Karlsruhe, D-76128 Karlsruhe, Germany

‡ Institute of Spectroscopy, Russian Academy of Sciences, Troitsk, Moscow region 142092, Russia

§ Institut des Materiaux de Nantes, F-44072 Nantes, France

Received 7 May 1997, in final form 7 August 1997

Abstract. We report on the polarized IR and Raman study of the misfit layer compound $(LaSe)_{1.14}(NbSe_2)_2$. The obtained data were compared with those obtained on the parent layer compounds LaSe and $NbSe_2$. On an assumption of a charge transfer of 1.14 electrons per formula unit from the LaSe to the $NbSe_2$ layers the decrease of the plasma frequency in the misfit compound with respect to that in the parent layer compounds is qualitatively explained. A qualitative model of electronic structure formation of the misfit layer compound from electronic bands of the parent layer compounds is discussed. An in-plane optical anisotropy related to the small misfit between the LaSe and $NbSe_2$ layer structures has been detected.

1. Introduction

From a general point of view misfit layer compounds of the type $(MX)_{1+y}(TX_2)_m$ consist of transition metal dichalcogenide layers TX_2 which are intercalated by non-transition metal chalcogenide MX layers [1–4]. Due to the different symmetry of the MX and TX_2 layers it results a misfit along one in-plane crystallographic axis even if along the perpendicular in-plane axis a perfect fit of both structures is accomplished [1]. This misfit is the reason for the deviation from the exact stoichiometric composition. In the special case of $(LaSe)_{1.14}(NbSe_2)_2$ (LNS) every intercalated LaSe (LS) layer is sandwiched by two 2H–$NbSe_2$ (NS) layers [2]. The sandwich unit is stabilized by a charge transfer from the LS layer to the adjacent NS layers. The LaSe subsystem obeys triclinic symmetry, while the structure of the $(NbSe_2)_2$ sandwich is determined by the $C222_1$ space group. The complete crystal is built up by a stack of sandwich units coupled by van der Waals bonds [5].

Vibrational and transport properties of misfit layer compounds studied by means of infrared and Raman spectroscopy have been reported earlier basically for the sulphur- (S-) based compounds [6–11]. Lattice dynamics peculiarities have been studied by Hangyo *et al* and Sourrisseau *et al*. The frequency shifts of the $(NbS_2)_2$ or $(TiS_2)_2$ sandwiches with respect to 2H–NbS_2 and 1T–TiS_2 respectively due to charge transfer from the MS layers to the Nb (Ti) ions have been found [6]. Some Raman bands in $(SnS)_{1.17}NbS_2$ and $(PbS)_{1.18}TiS_2$ were assigned to the incommensuration-mediated zone-folded acoustical modes [7]. The strength of the interlayer interaction has been discussed on the base of spectroscopic studies [8].

The optical reflectivity spectra were examined for a number of $(MS)_xTS_2$ (M = Sn, Pb, La, Sm, Tb; T = Nb, Ta) [8–11]. From plasma reflection and the high-frequency dielectric

0953-8984/97/4710545+09$19.50

constant the effective mass of the charge carriers has been estimated to be $m^* \simeq 0.3\,m_e$ for $(CeS)_{1.2}NbS_2$ [11] while $m^* \simeq 2.3\,m_e$ for $(PbS)_{1.14}NbS_2$ [9]. It is remarkable that the in-plane anisotropy of the plasma frequency ω_p is different for the two above-mentioned compounds: $\omega_p^a < \omega_p^b$ for the former compound, while for the latter one $\omega_p^a > \omega_p^b$. Hence, the influence of the incommensuration on the dynamics of free carriers in the misfit compounds is not very well understood.

We believe that the spectroscopic study of the Se-based misfit compounds may provide complementary information for understanding of the role of both the layered structure and the incommensuration in the lattice and free carrier dynamics.

In an earlier paper we have presented the first optical investigations on misfit layer compounds $(LnX)_{1+y}(NbX_2)_2$ (Ln ≡ Y, La or Nb; X ≡ S or Se) [12]. In the present work we report on improved optical data on LNS obtained on freshly cleaved (001) surfaces which reveal the optical in-plane anisotropy due to the misfit along the *a* axis. In addition we have investigated the optical properties of $NbSe_2$. Using further the reflectance spectrum of LaSe reported earlier [13], we have compared the experimental dielectric function of LNS with that for the LS and NS compounds and analysed the difference between them. On that basis and using the Raman data for LNS we argue that the LNS layer misfit compound is very similar to a metal–insulator quantum well system.

2. Experimental details

The misfit compound LNS is obtained from the elements by heating in an evacuated quartz tube. Details of crystal growth are described elsewhere [3]. The single crystals are platelets with a maximum size of $3 \times 5 \times 0.05$ mm^3. They can easily be split, resulting in well reflecting but wavy surfaces. Reflection measurements were performed at near-normal incidence on freshly cleaved (001) surfaces using a single-beam setup designed for the investigation of small samples. The energy range was varied between 50 meV and 6 eV. The electric field of incident light was polarized parallel to the *a* or *b* axis.

Raman spectra of the LNS crystals have been measured by means of a home-made multichannel spectrometer with a triple monochromatization at the spectral resolution about 3 cm^{-1}. The spectra were excited with the 514.5 nm line of an argon laser at grazing incidence and at a power density less than 50 W cm^{-2}. We have obtained the spectra in parallel (*aa* or *bb*) and crossed (*ab*) polarizations of the exciting and scattered radiations (*a* and *b* are the crystallographic axes within the layer plane of LNS and the *a* axis we associate with the misfit direction).

3. Results and discussion

3.1. IR spectra

The reflectance spectra $R_{\|a}$ and $R_{\|b}$ of LNS are shown in figure 1. They are characterized by a well pronounced plasma edge with spectral position around 0.7 eV and values of about 90% for the reflectivity at low energy, typical features of metallic behaviour. Compared to the previous results [12] the reflectance values in the UV region are significantly enhanced due to the high quality of the freshly cleaved surface. Additionally, the spectra reveal a small optical in-plane anisotropy between the orientation of the electric field parallel and perpendicular to the misfit axis.

For comparison the reflectance spectra of LS, NS and LNS obtained on (001) surfaces are plotted in figure 2. Whereas the LS and NS crystals do not show optical in-plane anisotropy

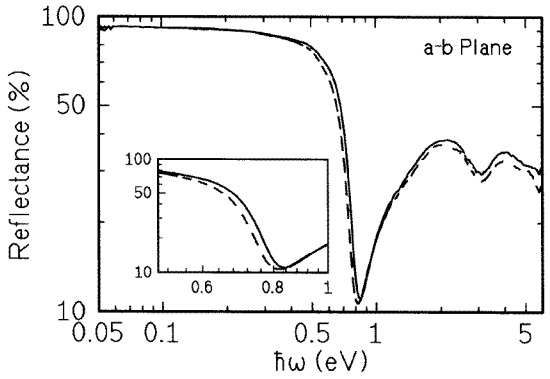

Figure 1. Polarized reflectance spectra of the (LaSe)$_{1.14}$(NbSe$_2$)$_2$ layer compound in the *a–b* plane. The misfit axis is not characterized directly, but one can consider it as an axis of lower plasma frequency (dashed line). The inset shows the anisotropy at the plasma edge in an expander scale.

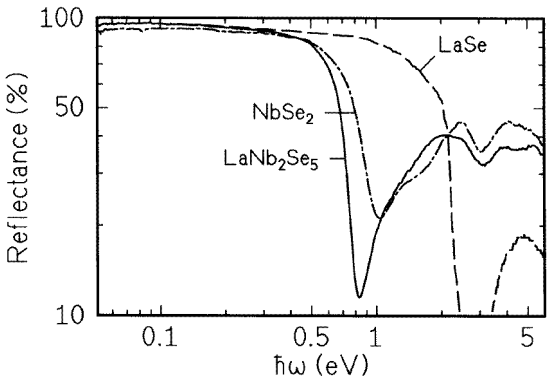

Figure 2. Unpolarized reflectance spectra of the single-layer compounds LaSe and 2H–NbSe$_2$ and the (LaSe)$_{1.14}$(NbSe$_2$)$_2$ crystal.

due to their crystal symmetry the reflectance spectrum of LNS in this figure corresponds to an average between $R_{\|a}$ and $R_{\|b}$. All crystals show metallic behaviour. Compared to the misfit compound the plasma edges of the parent layer compounds are shifted to higher energy. This indicates a decrease of carrier concentration if LS and NS are synthesized into the misfit LNS compound. For a quantitative analysis of the optical data the spectral distribution of the real and the imaginary part of the dielectric function was determined by fitting a Lorentz–Drude model to the reflectance spectra of figure 2. The results obtained for the in-plane tensor components of the conductivity function $\sigma_{\perp c} = \epsilon_0 \omega \epsilon_2$ are plotted in figure 3. This figure shows that the contributions of free carrier absorption and interband transitions are well separated. The spectral weight of the free carriers $W = \int \sigma_{FC}(\omega)\,\mathrm{d}\omega$ is reduced by about 50% in the misfit compound with respect to the values of both pristine compounds. In the region of interband transitions (> 1 eV) the situation is different. The absorption spectrum of LNS has a similar shape as the spectrum of the NS crystal. It contains, however, only two-thirds of the spectral weight of this parent compounds. In comparison to these compounds the spectral weight of the intrinsic absorption of LS below

3 eV can be neglected and even between 3 and 6 eV it is of minor importance. These features suggest the following model for the synthesis of the pristine compounds LS and NS to the misfit compound LNS (figure 4). Starting from the well known electronic structure of NS with a half-filled d_{z^2} conduction band [5], and a likewise half-filled d subband in LS, the preparation of the sandwich structure NS–LS–NS results in a complete charge transfer of the free carriers of LS, where they are distributed symmetrically amongst the two adjacent layers. By this charge transfer of 1.14 e^- per unit cell the intercalated LS layer becomes insulating and nearly transparent where the occupation of the half-filled d_{z^2} conduction band of the adjacent NS layers is increased by the charge transfer to an occupation of 78.5% resulting in p-type conduction. Consequently, the free carrier concentration in the sandwich is reduced compared to the value of pristine NS. This is reflected by the red shift of the plasma edge and the decrease of spectral weight W of the misfit compound in comparison to the NS crystal. The conception of the NS layers as the charge carrying network of LNS with a reduced carrier concentration is supported by the superconducting properties with values of $T_c = 5.3$ K for the misfit compound [14] and $T_c = 7.2$ K for pristine NS [15]. Similar considerations, as given here, were applied to explain the transport properties of the isoelectronic misfit compound $(CeS)_{0.6}NbS_2$ [11] and other S-based misfit compounds [8–10].

Table 1. Electronic conductivity spectrum parameters of $(LaSe)_{1.14}(NbSe_2)_2$ crystal.

	$\hbar\omega_p$ (eV)	$1/\tau$ (10^{14} s^{-1})	σ_0 (S cm^{-1})	N (10^{21} cm^{-3})	m^*/m_0	$\int \sigma_{FC}\, d\omega$
LaSe [4]	3.69	3.04	9147	18.4	1.86	190
$NbSe_2$	3.35	3.04	7539	15	1.84	130
$(LaSe)_{1.14}(NbSe_2)_2$	2.3	1.44	7502	4.56	1.19	90

The values of the plasma energy $\hbar\omega_p$ and of the scattering rate $1/\tau$ obtained from the Lorentz–Drude fit are used to calculate the effective mass m^* and the dc conductivity according to the relations

$$\omega_p^2 = \frac{Ne^2}{\epsilon_0 m^*} \tag{1}$$

and

$$\sigma = \omega_p^2 \epsilon_0 \tau \tag{2}$$

where N is the free carrier concentration determined from the stoichiometric composition. All results are compiled in table 1. The decrease of m^* in LNS compared to its value for NS can be qualitatively but not quantitatively explained in the framework of a rigid two-dimensional tight-binding model where the increase of the Fermi level from a half-filled to a more than three-quarter-filled band results in a decrease of the effective mass. An additional effect decreasing the effective mass will be discussed below.

As mentioned above the main features of the interband absorption in LNS are similar to those for the pristine compound NS (see figure 3). There are, however, some distinct differences compared to NS: the reduced spectral weight, the red shift of the absorption edge and the absorption peaks and, finally, a pronounced broadening of the absorption peaks. The loss of spectral weight of the sandwiched compound is due to the near-transparent insulating LS layers. The red shift of the absorption peaks indicates a decrease of the energy gap between valence and conduction band whereas broadening of the bands can account for the significant broadening of the absorption peaks. As the broadening implies an increased

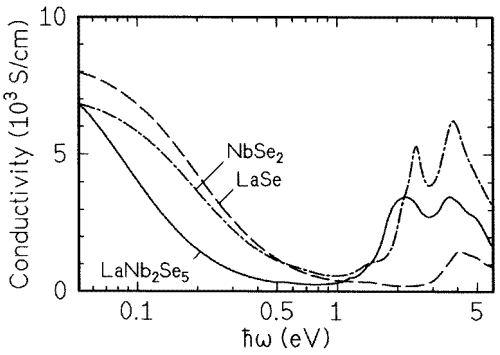

Figure 3. Unpolarized optical conductivity of the single-layer compounds and the (LaSe)$_{1.14}$(NbSe$_2$)$_2$ crystal calculated from the corresponding reflectivity spectra from figure 2.

dispersion of the conduction band, it contributes also to the decrease of the effective mass obtained for the transport properties of the sandwiched compound (see table 1).

After discussing the main electronic features of LNS we will turn to the small in-plane anisotropy manifested in figure 1 by the splitting of the plasma edge and small differences in the interband absorption. A comparison between the corresponding conductivity functions $\sigma_{\|a}$ and $\sigma_{\|b}$ reveals lower values of spectral weight for the electric field parallel to the misfit axis in the intraband as well as in the interband transition region (figure 5). According to the relation $\int \sigma_{FC}(\omega)\,\mathrm{d}\omega = \frac{1}{8}\omega_p^2$ the difference in spectral weight of the free carrier contribution can be expressed by an in-plane anisotropy of the effective mass tensor $m_{\|b}/m_{\|a} = 0.9$. The small anisotropy of the effective mass has also been observed earlier for the $(MS)_xTS_2$ (M = Sn, Pb, La, Sm, Tb; T = Nb, Ta) misfit layer compounds [9, 10]. The obtained values for the in-plane tensor components of the transport parameters of LNS are compiled in table 2.

3.2. Raman spectra

Polarized Raman spectra of LNS are shown in figure 6. In the parallel polarizations *aa* and *bb* the totally symmetric vibrations are Raman active. Figure 6 shows that the *aa* and *bb* spectra are very similar. The similarity between *aa* and *bb* spectra gives evidence for a weak anisotropy within the layer plane. The *ab* spectrum shows an essentially different form that is probably due to the predominant activity of nonsymmetric modes in this geometry.

Table 2. Anisotropy of electronic parameters of (LaSe)$_{1.14}$(NbSe$_2$)$_2$ crystal within the basal plane.

	$\hbar\omega_p$ (eV)	$1/\tau$ (10^{14} s^{-1})	σ_0 (S cm^{-1})	N (10^{21} cm^{-3})	m^*/m_0
(LaSe)$_{1.14}$(NbSe$_2$)$_2$ $\|$ *a*	2.24	1.44	7090	4.56	1.25
(LaSe)$_{1.14}$(NbSe$_2$)$_2$ $\|$ *b*	2.36	1.44	7870	4.56	1.12

As has been pointed out the crystal structure of LNS is built up of NS layers intercalated by LS layers so the structural unit is NS–LS–NS. The distance between the La atom and the nearest Se atom from the NS layer is approximately the same as the La–Se distance inside the LS layer (averaged distance is about 3.05 Å). This suggests that the layers LS and NS

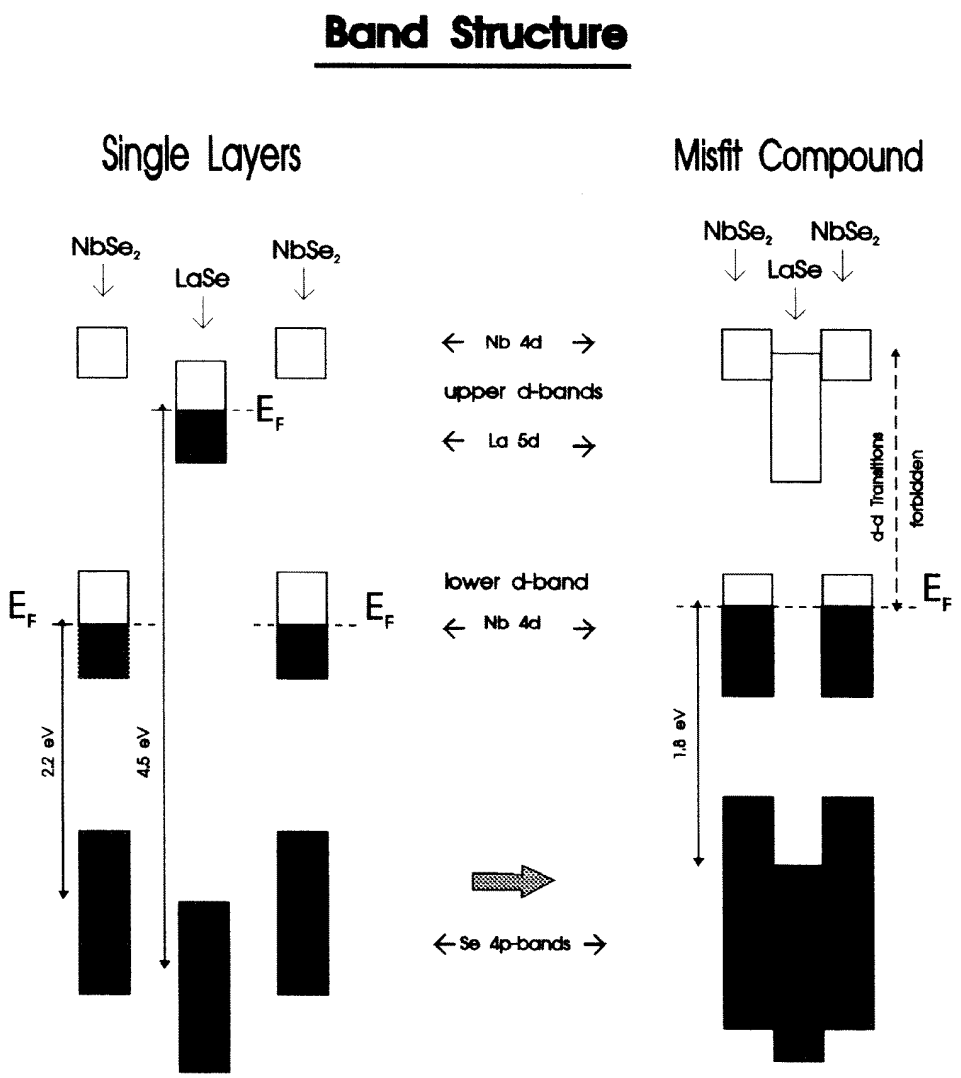

Figure 4. Hypothetical band structure of the LN and NS single-layer and $(LaSe)_{1.14}(NbSe_2)_2$ misfit compounds.

are linked most likely by strong bonding. The sandwiches NS–LS–NS similar to the NS layers in 2H–$NbSe_2$ are linked by the van der Waals bonds. The unit cell of LNS contains two sandwiches. On the other hand, the LNS structure can be considered as a superlattice consisting of –NS–LS–NS–NS–LS–NS– layers with the period of 36.5 Å. Therefore it is expedient to compare the spectra of LNS and that of NS for an interpretation of the LNS Raman spectra.

The NS crystal contains two layers in the unit cell and normal modes have the following irreducible representations at the Γ point [16]

$$A_{1g} + 2B_{2g} + E_{1g} + 2E_{2g} + 2A_{2u} + B_{1u} + 2E_{1u} + E_{2u}$$

where the $A_{1u} + E_{2u}$ modes are acoustical and $B_{2g} + E_{2g}$ are interlayer modes corresponding

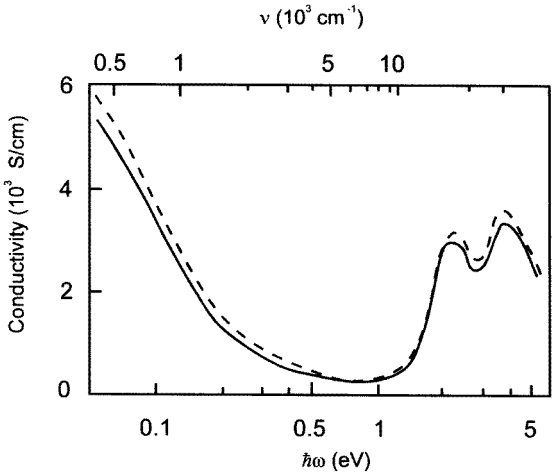

Figure 5. Polarized conductivity spectra of the (LaSe)$_{1.14}$(NbSe$_2$)$_2$ layer compound in the *a–b* plane. Solid curve corresponds to $E \parallel a$ and dashed curve corresponds to $E \perp a$ (*a* is assumed to be the misfit axis).

to rigid layer vibrations. We will discuss only intralayer vibrations because of lack of complete information about interlayer modes. Only two modes among four intralayer $A_{1g} + B_{2g} + E_{1g} + E_{2g}$ modes have been revealed at 230 cm^{-1} (A_{1g}) and 238 cm^{-1} (E_{2g}) [17–19]. Besides, the intense broad line at 180 cm^{-1} assigned to the LA overtone has also been reported.

The spectra of the LNS crystal differ substantially from those of the NS crystal. The former reveal more lines than can be expected from an increased number of NS layers in the unit cell of LNS. In particular, the broad line near 200 cm^{-1} we ascribe to two-phonon scattering similar to that observed in NS at 180 cm^{-1}. The higher intensity of this band in the *aa* spectrum compared to that in the *bb* spectrum can be related to the small in-plane anisotropy shown in figure 1. The other lines in figure 6 should be attributed to one-phonon spectrum. We attribute the lines at frequencies above 200 cm^{-1} to vibrations of atoms in the NS layer while those below 200 cm^{-1} to intralayer vibrations of LS layers. This assignment is based upon the fact that all the intralayer modes of the NS crystal are located above 200 cm^{-1} [17–19].

Table 3. Frequencies (in cm^{-1}) of the normal modes in the layered crystals.

Crystals	A_{1g}	E_{1g}	B_{2g}	E_{2g}
MoS_2	409	287	475	383
2H–$NbSe_2$	230	—	—	238
(LaSe)$_{1.14}$(NbSe$_2$)$_2$ crystal	286	225	320	250

The assignment of lines attributed to intralayer modes of the NS layer in the LNS spectra and a comparison with corresponding modes for NS and MoS_2 crystals are given in table 3. It is seen that frequencies of modes in LNS are higher than those of corresponding modes for NS. This gives evidence for decrease of interatomic distances in NS layers of the LNS crystal in accordance with x-ray data.

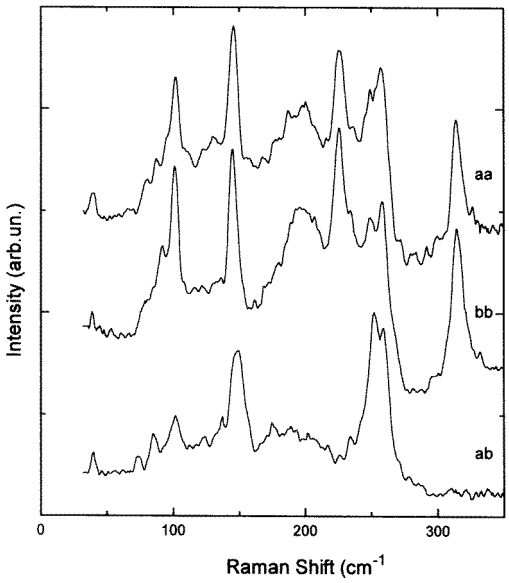

Figure 6. The polarized Raman spectra of the $(LaSe)_{1.14}(NbSe_2)_2$ crystal in the parallel (*aa* or *bb*) and crossed (*ab*) polarizations of exciting and scattered radiation.

The 102 and 148 cm^{-1} bands can be assigned to vibrations of atoms within the LS layer. The LS crystal has f.c.c. structure of the NaCl type [20]. The vibrational spectrum of this crystal should consists of one TO mode and a doubly degenerate LO mode, both Raman inactive. The LS layer in LNS loses its centrum of symmetry and the above-mentioned modes may become Raman active.

Hence, we assume that the optical phonon frequencies for the NS and LS layers do not overlap in the LNS spectrum. This may give rise to mode confinement within each layer, as happens in superlattices [21]. Usually this effect manifests itself in the appearance of additional lines in the spectrum due to the Brillouin zone folding, that has been recently discussed for LA and TA type modes in $(SnS)_{1.17}NbS_2$ and $(PbS)_{1.18}TiS_2$ [7]. It is more notable for modes with strong dispersion. One can see from figure 6 that the 102 and 148 cm^{-1} modes are accompanied by low-frequency shoulders, that possibly can be related to the mode confinement.

4. Conclusions

The electronic properties of the sandwich compound $(LaSe)_{1.14}(NbSe_2)_2$ can be treated as being composed of the electronic properties of the pristine compounds LaSe and $NbSe_2$ taking into account a complete charge transfer of the free carriers of the intercalated LaSe layer to the adjacent $NbSe_2$ layers. Additionally, the properties of the sandwich unit consisting of a nearly transparent and insulating LaSe and two adjacent metallic $NbSe_2$ layers show some minor modifications: a broadening of valence and conduction bands, a slight decrease of the band gap and small in-plane anisotropy due to crystallographic misfit. One might speculate that the $(LaSe)_{1.14}(NbSe_2)_2$ misfit compound as well as the S-based misfit compounds are natural metal–insulator quantum well systems.

Acknowledgments

This work was supported by the European Communities under contract No CI1-0526-M(CD), by the Deutsche Forschungsgemeinschaft and by the Russian Foundation for Basic Research (grant No 96-02-18114). One of the authors (VMB) gratefully acknowledges financial support of the Deutsche Forschungsgemeinschaft during his stay at the Institut für Angewandte Physik, Universität Karlsruhe.

References

[1] Wiegers G A 1996 *Prog. Solid State Chem.* **24** 1
[2] Roesky R, Meerschaut A, Rouxel J and Chen J 1993 *Z. Anorg. (Allg.) Chem.* **619** 117
[3] Roesky R 1994 *PhD Thesis* University of Nantes
[4] Zhuze V P, Karin M G, Lukirskil D P, Sergeeva V M and Shelykh A I 1980 *Sov. Phys.–Solid State* **22** 1558
[5] Mattheiss L F 1973 *Phys. Rev.* B **8** 3719
[6] Hangyo M, Nakashima S, Hamada Y, Nishio T and Ohno Y 1993 *Phys. Rev.* B **48** 11 291
[7] Sourisseau C, Cavagnat R and Tirada J L 1992 *J. Raman. Spectrosc.* **23** 647
[8] Hangyo M, Nishio T, Nakashima S, Ohno Y, Terashima T and Kojima M 1993 *Japan. J. Appl. Phys.* **32** (Supplement 3) 581
[9] Rüscher C H, Haas C, van Smaalen S and Wiegers G A 1994 *J. Phys.: Condens. Matter* **6** 2117
[10] Rüscher C H 1996 *Phys. Status Solidi.* b **198** 889
[11] Terashima T, Kojima N, Okamoto H and Mitani T 1993 *J. Phys. Soc. Japan* **6** 2166
[12] Roesky R, Gressier P, Meerchaut A, Widder K, Geserich H P and Scheiber G 1994 *J. Phys.: Condens. Matter* **6** 3437
[13] Ettema A R H F, van Smaalen S, Haas C and Turner T S 1994 *Phys. Rev.* B **49** 10 585
[14] Fisher W G and Sienko M J 1980 *Inorg. Chem.* **19** 39
[15] Revolinsky E, Coleman G A and Beerntsen D J 1969 *J. Chem. Phys. Solids* **26** 193
[16] Wieting T J 1973 *Solid State Commun.* **12** 931
[17] Wang C S and Chen J M 1975 *Solid State Commun.* **14** 1145
[18] Tsang J C, Smith J and Shafer M F 1976 *Phys. Rev. Lett.* **37** 1407
[19] Klein M V 1982 *Light Scattering in Solids III (Topics Appl. Phys. 51)* ed M Cardona and G Güntherodt (Berlin: Springer)
[20] Gerhard C, Hiltrud H and Ingeborg H (eds) 1983 *Gmelin Handbook* vol 15 (Berlin: Springer) p 39
[21] Cardona M 1989 *Superlatt. Microstruct.* **5** 27